Journal of Materials in Civil Engineering. Submitted November 20, 2012; accepted March 25, 2013; posted ahead of print April 1, 2013. doi:10.1061/(ASCE)MT.1943-5533.0000824

Resilient Modulus and Permanent Deformation Responses of Geogrid-Reinforced Construction and Demolition Materials

M.A. Rahman[1]; A. Arulrajah[2]; J. Piratheepan[3]; M.W. Bo, M.ASCE[4]; and M.A. Imteaz[5]

[1]PhD Student, Faculty of Engineering & Industrial Sciences, Swinburne University of Technology. mdaminurrahman@swin.edu.au.

[2]Associate Professor, Faculty of Engineering & Industrial Sciences, Swinburne University of Technology, aarulrajah@swin.edu.au.

[3]Lecturer, Faculty of Engineering & Industrial Sciences, Swinburne University of Technology. pjegatheesan@swin.edu.au.

[4]Senior Principal/Director, DST Consulting Engineers Inc., Thunder Bay, Ontario, P7B 5V5, Canada. mwinbo@dstgroup.com.

[5]Senior Lecturer, Faculty of Engineering & Industrial Sciences, Swinburne University of Technology. mimteaz@swin.edu.au.

Journal of Materials in Civil Engineering. Submitted November 20, 2012; accepted March 25, 2013;
posted ahead of print April 1, 2013. doi:10.1061/(ASCE)MT.1943-5533.0000824

Abstract

Extensive amounts of natural quarry aggregates are currently being used in road and pavement applications. The use of construction and demolition (C&D) materials such as recycled concrete aggregate (RCA), crushed brick (CB) and reclaimed asphalt pavement (RAP) as an alternative to quarry aggregates has generated interest in recent years, particularly as a pavement base or subbase material. However, the resilient moduli responses and performance of these C&D materials reinforced with geogrids under repeated loads has yet to be established. This research investigates the resilient moduli (M_R) and permanent deformation characteristics of C&D materials reinforced with biaxial and triaxial geogrids with the use of a repeated load triaxial (RLT) equipment. The effects of varying deviatoric stress on the resilient modulus of unreinforced and geogrid-reinforced C&D materials were also investigated. Regression analyses of resilient modulus test results were performed using the two and three-parameter models. The M_R properties of the geogrid-reinforced RCA and CB were found to be higher than that of the respective unreinforced material. The M_R value of RCA+Biaxial increased by 24% and of RCA+Triaxial increased by 34% when compared with unreinforced RCA. The permanent deformation value obtained from RCA+Biaxial decreased by 29% and of RCA+Triaxial decreased by 36% when compared with unreinforced RCA. The M_R value of CB+Biaxial increased by 16% and of CB+Triaxial increased by 55% when compared with unreinforced CB. The permanent deformation value decreased by 29% and 37% for CB+Biaxial and CB+Triaxial respectively when compared with unreinforced CB material. The incorporation of geogrids was found to have significant effects on the resilient modulus and permanent deformation characteristics of C&D materials. The three parameter resilient moduli model was found to provide a good fit for the geogrid-reinforced C&D materials.

Keywords: Geogrids; recycled materials; resilient modulus; geotechnical; demolition.

Journal of Materials in Civil Engineering. Submitted November 20, 2012; accepted March 25, 2013;
posted ahead of print April 1, 2013. doi:10.1061/(ASCE)MT.1943-5533.0000824

Introduction

Quarry aggregates are increasingly being used in civil engineering applications such as backfilling, embankments, road bases, road subbases, slope stabilisation and footpaths. As a result, large quantities of virgin natural aggregate resources are being consumed in these applications. Subsequently, large amount of waste materials are being generated which imposes significant pressure on landfill facilities and the environment (Aatheesan et al. 2010; Hoyos et al. 2011; Arulrajah et al. 2012a). A significant proportion of these waste materials are produced from the Construction and Demolition (C&D) sectors, a large part of which is primarily obtained from demolished buildings and infrastructure (Apotheker 1990; Gavilan and Bernold 1994). Recycling of C&D waste materials into sustainable civil engineering applications is of global importance, as we seek new ways to conserve our natural resources as well as reduce reusable waste materials from being landfilled (Arulrajah et al. 2012b).

The viability of using various C&D materials in civil engineering applications such as pavement and road construction applications have been recently investigated by several researchers. These include C&D materials such as RCA (McKelvey et al. 2002; Poon and Chan 2006a, 2006b; Debieb and Kenai 2008; Arulrajah et al. 2012c; Azam and Cameron 2012; Gabr and Cameron 2012), CB (Aatheesan et al. 2010; Arulrajah et al. 2011a; Arulrajah et al. 2012a; Piratheepan et al. 2013), RAP (Taha et al. 2002; Han et al. 2011; Hoyos et al. 2011; Puppala et al. 2011; Thakur et al. 2012) and recycled glass (Ali et al. 2011; Disfani et al. 2011; Arulrajah et al. 2012d; Disfani et al. 2012; Imteaz et al. 2012). Among the C&D materials, RCA, CB and RAP are the most commonly used in civil engineering applications particularly due to their higher strength properties, durability and availability.

Journal of Materials in Civil Engineering. Submitted November 20, 2012; accepted March 25, 2013; posted ahead of print April 1, 2013. doi:10.1061/(ASCE)MT.1943-5533.0000824

Several researchers have also evaluated the sustainable usage of other forms of waste materials which includes waste excavation rock (Arulrajah et al. 2012e), quarry wastes (Liu et al. 1998; Goodhue et al. 2000; Huang et al. 2002; ; Chung and Lo 2003; Bianchini et al. 2005; Rao et al. 2007; Tam and Tam 2007), recycled ballast (Indraratna et al. 2002, 2003, 2005) and wastewater biosolids (Arulrajah et al. 2011b, 2013a) in pavement sub-base and road applications, which is an indication of increasing global interest in the sustainable usage of recycled waste materials in civil engineering applications.

The reinforcement of C&D aggregates with geogrids in civil engineering applications will further increase the usage of C&D aggregates in various applications as a result of the enhanced strength and resilient modulus properties. The interaction mechanisms between geogrids with soils or aggregates provides frictional resistance between the soil and the surface of the geogrids as well as internal shear resistance of the soil and passive resistance of the transverse ribs (Alfaro et al. 1995; Tatlisoz et al. 1998; Mengelt et atl. 2000; Liu et al. 2009a; Liu et al. 2009b).

Abu-Farsakh et al. (2007), Chen et al. (2012) and Arulrajah et al (2013b) have undertaken resilient modulus and permanent deformation testing of recycled aggregates as well as geogrid-reinforced quarry aggregates using repeated the load triaxial (RLT) equipment. Chen et al. (2012) reported that the inclusion of geogrid reinforcement had significant effects on the resilient modulus and permanent deformation characteristics of crushed limestone pavement base materials, whereby M_R was found to increase and permanent deformation decrease with the incorporation of geogrids.

Journal of Materials in Civil Engineering. Submitted November 20, 2012; accepted March 25, 2013; posted ahead of print April 1, 2013. doi:10.1061/(ASCE)MT.1943-5533.0000824

The main objective of this research is to evaluate the resilient moduli responses of C&D materials reinforced with geogrids under repeated loading when used in pavement base/subbase applications. Regression modelling and structural layer coefficient of geogrid-reinforced C&D materials were analyzed in this research. The C&D materials investigated were unreinforced as well as geogrid-reinforced RCA and CB materials.

Experimental Procedure

The C&D materials were collected from a recycling site in Melbourne, Australia. The maximum particle size of the C&D materials was 19 mm. The samples were first oven dried at 60˚C until fully dried for various laboratory experiments. Commercially available biaxial geogrids (Biaxial) with an ultimate tensile strength of 20 kN/m and triaxial geogrids (Triaxial) with ultimate tensile strength of 32 kN/m were used in the tests. The Biaxial geogrid had square shaped apertures with aperture dimensions of 39mm x 39mm. The Triaxial geogrid had triangular shaped apertures with aperture dimensions of 46mm x 46mm x 46mm. The geogrids were manufactured from polypropylene polymers. The physical properties tests such as modified compaction test, specific gravity, particle size distribution, water absorption, Los Angeles abrasion were undertaken on the C&D materials.

Modified compaction tests were conducted according to ASTM D1557-(2009) to determine the maximum dry density and optimum moisture content of the samples. As the maximum particle size was of 19 mm, a cylindrical mould having an internal diameter of 152.4 mm was used. The samples were compacted in five layers and each layer by 56 blows of 4.9 kg rammer falling freely from 450 mm in height.

Journal of Materials in Civil Engineering. Submitted November 20, 2012; accepted March 25, 2013; posted ahead of print April 1, 2013. doi:10.1061/(ASCE)MT.1943-5533.0000824

The particle size distribution of C&D materials were conducted by sieve analysis according to ASTM D422-63 (2007), which is similar to AS 1141.11 (SAA 1996). The particle size distribution for C&D materials targeted lower and upper bound reference lines for aggregates in pavement subbase applications (Aatheesan et al. 2010; Arulrajah et al. 2011a; Arulrajah et al. 2012a). Initially the samples were cleaned with distilled water by using sieve size of 75 μm. The retained sample was taken and dried for 24 hours before further sieve analysis tests. CBR tests were carried out according to ASTM D1883 (2007) on specimens subjected to modified Proctor compaction effort at the optimum water content and soaked for 4 days to simulate the worst-case scenario. In the modified CBR tests, samples were placed in a cylindrical mould (internal diameter of 152 mm) and compacted in five layers totalling an effective height of 117 mm by inserting a spacer disc into the mould before compaction. Modified compaction effort was used.

Organic content tests were performed in accordance with ASTM D2974 (2007). The ignition method was used to determine the organic content of the samples. Specific gravity and water absorption tests of coarse aggregate (retained on 4.75 mm sieve) and fine aggregate (passing through 4.75 mm sieve) were carried out according to AS1141.5 (SAA 2000a) and AS1141.6.1 (SAA 2000b), respectively. Flaky characteristics of the samples were determined by flakiness index test according to BS 812-105.1 (BSI 2000) on oven dry samples. The Los Angeles abrasion test was conducted according to ASTM C131 (2006) to determine the resistance of aggregate by abrasion and impact forces.

The M_R tests were undertaken by using RLT equipment to simulate the traffic wheel loading on base/subbase by applying cyclic loading on the specimens as per AASHTO T307 (2003) standard. In this method a haversine-shaped wave load pulse was applied with a loading

Journal of Materials in Civil Engineering. Submitted November 20, 2012; accepted March 25, 2013;
posted ahead of print April 1, 2013. doi:10.1061/(ASCE)MT.1943-5533.0000824

period of 0.1 second and a resting period of 0.9 second. Unreinforced and geogrid-reinforced C&D materials were tested with the RLT equipment at the optimum moisture content. Each specimen was subjected to five different confining stresses and three different deviatoric stresses at each confining stress. Pneumatic pressure was used for the confining and deviator stress, which were computer controlled. Oven dried C&D samples were prepared in a split mould of 100 mm diameter and 200 mm of height. The geogrid-reinforced specimens were prepared with the geogrid placed in the middle of the specimen (at the specimen height of 100 mm). The samples were mixed with water to their optimum moisture content and kept for 24 hours in a closed container. The samples were next compacted to their maximum dry density with modified compaction effort. Two saturated porous disc were placed at the bottom and top of the sample. A rubber membrane was used over the sample and two O-rings were also placed to the pedestal and the top loading cap. M_R tests were then undertaken on the sample. To evaluate permanent deformation of the unreinforced and geogrid-reinforced samples, separate specimens were prepared and tested.

Results and Discussion

The physical properties of C&D materials obtained from the laboratory tests are presented in Table 1. As the RAP specimens failed during RLT testing after just a few load cycles, due to a lack of cohesion in this material, the RAP results are not discussed further. The particle-size distribution results for C&D materials undertaken before compaction with modified compaction effort, is shown in Fig. 1. The particle size distribution curves for the C&D materials were consistent with the requirements of typical aggregates in civil engineering applications such as pavements and footpaths (Aatheesan et al. 2010; Arulrajah et al. 2011a). The gravel, sand and fine contents of the C&D materials obtained from sieve analysis are presented in Table 1. Often road authorities specify limits of acceptable values for coarse and

Journal of Materials in Civil Engineering. Submitted November 20, 2012; accepted March 25, 2013; posted ahead of print April 1, 2013. doi:10.1061/(ASCE)MT.1943-5533.0000824

fine aggregates and as such these properties have been reported where relevant in the table. The coefficient of uniformity (C_u) and coefficient of curvature (C_c) values indicates that the C&D materials satisfy the criteria typically specified of having $C_u > 4$ and $1 < C_c < 3$.

The specific gravity of coarse aggregates (retained on 4.75 mm sieve) is generally higher than that of fine aggregates (passing 4.75 mm sieve). The specific gravity of the C&D materials indicate that they can be considered as high quality aggregates. The water absorption of fine particle is greater than coarse particle as the fine particle absorb more water, except CB materials. The organic content of the C&D materials was low. The flakiness index values were within the upper limit value of 35; typically specified for pavement base or subbase materials. The Los Angeles abrasion loss result indicates that the C&D aggregates are durable with results within the upper limit value of 40; typically adopted by road authorities for pavement base or subbase materials. The CBR test results for RCA and CB were found to be within the typical values of 80-120, which are normally specified for pavement base and subbase applications (Arulrajah et al. 2012a; Arulrajah et al. 2012b). The modified compaction tests were carried out on C&D materials which indicated that the maximum dry density and optimum moisture content was consistent with that of typical construction aggregates (Arulrajah et al. 2012b).

The M_R test results for unreinforced and geogrid reinforcement with biaxial and triaxial geogrids for RCA and CB materials are presented in Figs. 2, 3 and 4, respectively. From these figures, it is observed that M_R value increased with an increase of axial stress and deviator stress. This may be attributed to the fact that with increasing confining stress, voids of the specimen decrease and specimen become denser and stiffer with a subsequent increase in M_R. The M_R value was consistently higher for unreinforced and geogrid-reinforced RCA

Journal of Materials in Civil Engineering. Submitted November 20, 2012; accepted March 25, 2013;
posted ahead of print April 1, 2013. doi:10.1061/(ASCE)MT.1943-5533.0000824

as compared to the corresponding CB materials for the various confining stresses, indicating RCA to be a higher quality material than CB. Reinforcement of RCA and CB with geogrids was found to result in improved stiffness properties.

Fig. 5 presents a comparison of M_R with deviator and confining stresses for unreinforced and geogrid-reinforced RCA aggregates. Effects of confining and deviatoric stresses on M_R can be clearly noticed in the figure. It is evident that M_R is higher for the geogrid-reinforced RCA as compared to unreinforced RCA. RCA+Triaxial had the highest M_R followed by RCA+Biaxial, which is mainly attributed to higher tension capacity of triaxial compared to biaxial geogrid. Other factors such as orientation of the apertures, rigid junctions and stiffer ribs can also contribute to the difference.

Fig. 6 presents a comparison of M_R with deviator and confining stress for unreinforced and geogrid-reinforced CB aggregate. It is again evident that M_R is higher for the geogrid-reinforced CB as compared to unreinforced CB. CB+Triaxial had the highest M_R followed by CB+Biaxial.

In Figures 5 and 6, M_R is observed to increase with an increase of deviator stress under the same confining stress. With an increase in deviator and confining stress, the M_R value increased considerably as the materials become stiffer with each cycle of deviatoric stress (Fang-Le and Jian-Zhong 2004). This higher M_R value is mainly attributed to the strain hardening behavior of unbound aggregate materials.

The M_R value obtained from unreinforced RCA was 330 MPa, which is consistent with the results reported previously by others (Maher et al. 1997; MacGregor et al. 1999; and

Journal of Materials in Civil Engineering. Submitted November 20, 2012; accepted March 25, 2013; posted ahead of print April 1, 2013. doi:10.1061/(ASCE)MT.1943-5533.0000824

Gnanendran and Woodburn 2003). The M_R value of RCA+Biaxial increased by 24% and of RCA+Triaxial increased by 34% when compared with unreinforced RCA at a maximum confining stress of 137.9 kPa. The permanent deformation value obtained from RCA+Biaxial decreased by 29% and of RCA+Triaxial decreased by 36% when compared with unreinforced RCA at a deviator stress of 150 kPa..

The M_R value obtained from unreinforced CB was 228MPa at 137.90 kPa confining stress. The M_R value of CB+Biaxial increased by 16% and of CB+Triaxial increased by 55% when compared with unreinforced CB at a maximum confining stress of 137.9 kPa. The permanent deformation value decreased by 29% and 37% for CB+Biaxial and CB+Triaxial respectively when compared with unreinforced CB material at a deviator stress of 150 kPa.

Reinforcement of RCA and CB with geogrids was found to result in improved stiffness properties as expected. The incorporation of geogrids in this research was found to have significant effects on the resilient modulus and permanent deformation characteristics of C&D materials. The RLT results are consistent with the findings of Chen et al. (2012) whom reported that the inclusion of geogrid reinforcement reduced the permanent deformation and increased the MR for crushed limestone pavement base materials. It is worth noting that several researchers (Moghaddas-Nejad and Small 2003, Perkins et al. 2003, and Nazzal et al. 2007) have on the other hand reported that geogrid reinforcement does not have significant effect on the resilient modulus and permanent deformation behavior of crushed limestone samples (Moghaddas-Nejad and Small 2003, Perkins et al. 2003, and Nazzal et al. 2007).

Journal of Materials in Civil Engineering. Submitted November 20, 2012; accepted March 25, 2013; posted ahead of print April 1, 2013. doi:10.1061/(ASCE)MT.1943-5533.0000824

Two-Parameter Model

The two-parameter or bulk stress model is a regression model used to analyze the M_R of granular materials (AASHTO T 307, 2003)**.** The two-parameter model can analyze confining and deviator stresses separately (Puppala et al. 2011). This model has been found to be reliable to determine the modulus properties of granular materials (Puppala et al. 2011). The two-parameter model is presented in the following equations (Puppala et al. 2011):

$$M_R = k_1 \times \theta^{k_2} \quad (1)$$

$$logM_R = logk_1 + k_2 \times log\theta \quad (2)$$

Where, M_R = resilient modulus; θ = bulk stress = $\sigma_1 + \sigma_2 + \sigma_3 = 3\sigma_3 + \sigma_d$; σ_1, σ_2 and σ_3 are the principle stress; σ_d is the deviator stress and k_1 & k_2 are the theta model parameters.

A statistical regression program was used for the determination of model parameters ($logk_1$ and k_2). The results obtained from the statistical analysis are presented in Table 2. Fig. 7 indicates that an excellent fit and a linear trend was obtained from the statistical analysis for the unreinforced and reinforced specimens. The theta parameter $logk_1$, is an indicator of M_R magnitudes (Puppala et al. 2011), varies from 0.26-0.38 for RCA aggregate and increases with the inclusion of geogrids. The theta parameter $logk_1$ for CB aggregate varies from 0.10-0.28 and also increases with the inclusion of geogrids. The k_2 parameter values also increased with the inclusion of geogrids for RCA and CB. The M_R value shows a linear trend whereby the k_2 parameter is close to 1, which is higher when compared with the unreinforced specimen.

Journal of Materials in Civil Engineering. Submitted November 20, 2012; accepted March 25, 2013;
posted ahead of print April 1, 2013. doi:10.1061/(ASCE)MT.1943-5533.0000824

Three-Parameter Model

The three-parameter model can analyze both confining and deviator stresses together (Puppala et al. 1997). The resilient modulus test results were analyzed by using the following model.

$$\frac{M_R}{\sigma_{atm}} = k_3 \times \left(\frac{\sigma_3}{\sigma_{atm}}\right)^{k_4} + \left(\frac{\sigma_d}{\sigma_{atm}}\right)^{k_5} \quad (3)$$

Where, M_R is the resilient modulus; k_3, k_4, k_5 are the three parameter model constants; σ_{atm} is the atmospheric pressure; σ_3 is the confining stress and σ_d is the deviator stress. The Matlab software was used to determine the three parameter constants in the model. The three-parameter model constants and coefficient values are presented in Table 3. From the table it is observed that the k_3 parameter varies from 0.81 to 1.10 for RCA aggregate and 0.75 to 1.04 for CB aggregate. The maximum value of k_3 was achieved from RCA+Triaxial and the lowest value obtained from unreinforced aggregate. The k_3 value increased with the inclusion of geogrids, for both RCA and CB aggregates which is considered suitable for pavement base/subbase applications. The k_4 parameter for RCA aggregate varies from 0.69 to 0.73 and for CB aggregate varies from 0.32 to 0.38. Table 3 also indicates that higher k_5 value of 0.15 is obtained from geogrid reinforced RCA aggregates as compared to the other specimens. The low value of 0.08 was obtained from unreinforced CB aggregates. The three parameter results indicate that geogrid reinforced RCA aggregate was a better quality material than reinforced CB. The results indicate that the three-parameter model provided a better fit for both confining and deviator stress in comparison with two-parameter model as this model has more than two constants and results obtained would be more accurate than the two parameter model.

Journal of Materials in Civil Engineering. Submitted November 20, 2012; accepted March 25, 2013; posted ahead of print April 1, 2013. doi:10.1061/(ASCE)MT.1943-5533.0000824

Structural Layer Coefficients

According to AASHTO (1993), layer coefficients can be measured from the M_R properties and used to estimate base or subbase layer thickness of flexible pavement. Hence in this research, layer coefficients were calculated from the average M_R at three different deviator stresses for each confining stress. According to AASHTO (1993) flexible pavement design guidelines layer coefficients are determined for base and subbase layer by using the following empirical relationships:

$$a_2 = 0.249 \times logM_R - 0.977 \quad (4)$$

$$a_3 = 0.227 \times logM_R - 0.839 \quad (5)$$

Where, a_2 is the base layer coefficient; a_3 is the subbase layer coefficient and M_R is the resilient modulus in psi. The structural layer coefficients for base and subbase layers are presented in Table 4 and Table 5.

Table 4 indicates that the base layer coefficient increased with the increase in confining stress and the maximum value of 0.205 was obtained at 137.90 kPa confining stress for RCA+Triaxial. Table 4 also indicates that the minimum base layer coefficient of 0.028 obtained from unreinforced CB aggregate at 20.70 kPa confining stress and maximum layer coefficient of 0.181 for CB+Triaxial aggregates at 137.90 kPa confining stress. Table 5 indicates that the subbase layer coefficient is found to increase with an increase of confining stress. The minimum a_3 value of 0.074 was obtained at 20.7 kPa confining stress for the unreinforced RCA and a maximum value of 0.239 was achieved for RCA+Triaxial at 137.90 kPa confining stress. Similar trend also observed for CB aggregates where the minimum subbase layer coefficient value of 0.03 was obtained at confining stress of 20.7 kPa for

Journal of Materials in Civil Engineering. Submitted November 20, 2012; accepted March 25, 2013; posted ahead of print April 1, 2013. doi:10.1061/(ASCE)MT.1943-5533.0000824

unreinforced CB aggregates and maximum value of 0.22 was achieved for CB+Triaxial at confining stress of 137.9 kPa. The results indicate that geogrid reinforced RCA aggregate would be a higher quality base and subbase materials rather than CB aggregate.

The layer coefficients are an indicator of strength and depend on the structural efficiency of the materials. In a typical multi-layered pavement structure, the base material has higher resilient modulus than the subbase material. As such a_2 (base layer coefficient) value is usually higher than a_3 (subbase layer coefficient). In this research study, the a_2 and a_3 values were calculated using the same resilient modulus (i.e. the base and the subbase layers with the same recycled C&D aggregate). For this reason, the obtained a_2 values are less than a_3. This would indicate that should this same recycled C&D aggregate is used in both the base and subbase layers the base layer materials should also be reinforced with geogrids, based on the layer coefficient values

Permanent Deformation Characteristics

The RLT testing equipment was used to determine the permanent strain of unreinforced and geogrid-reinforced C&D materials. Three different deviatoric stresses (150kPa, 250kPa and 350kPa) and a constant confining stress (50kPa) were used for the permanent deformation tests according to Austroads (2004) over 30,000 loading cycles. The results of permanent strain for the unreinforced and geogrid-reinforced RCA and CB are presented in Fig. 8 and Fig. 9, respectively while the final deformation values at 30,000 cycles of unreinforced and reinforced RCA and CB aggregates are presented in Table 6. The results from Fig. 8 and Fig. 9 show that permanent strain increased with increasing deviator stresses for constant confining stress. After a certain number of load cycles the curve flattened to horizontal straight line at the lower deviator stresses with the exception of 350 kPa, where the sample failed prior to completion of the load cycle of 30000 for both RCA and CB. This is attributed

Journal of Materials in Civil Engineering. Submitted November 20, 2012; accepted March 25, 2013; posted ahead of print April 1, 2013. doi:10.1061/(ASCE)MT.1943-5533.0000824

to the fact that the material responses had become resilient with increasing load cycles at these lower deviator stresses. Arulrajah et al. (2011a) reported a similar trend of results in their research on unreinforced recycled brick. It is also observed in the figures that the permanent strain for unreinforced RCA and CB is higher than that of the geogrid-reinforced RCA and CB. The RCA+Triaxial and CB+Triaxial specimens exhibited lower permanent strain as compared to the corresponding Biaxial and unreinforced materials.

Permanent deformation results can be presented in terms of the relationship between permanent strain rate and permanent strain (Dawson and Wellner 1999). Permanent strain rate versus permanent cumulative strain of the unreinforced and geogrid-reinforced RCA and CB are shown in Fig. 10 and Fig. 11, respectively for 150kPa, 250kPa and 350kPa deviator stresses. According to Austroads (2004) and Korkiala and Dawson (2007), the permanent deformation profile consists of three different stages: primary, secondary and final stage. The primary stage lasts for only a few hundred cycles and is followed by the secondary stage consisting of several hundred to several millions of cycles. The responses of all materials were plastic in the first and second stages for a finite number of load applications, but after completion of the post compaction period, the response becomes entirely resilient, and no further permanent strain occurred. In the third stage, the strain rate for all the materials continued to increase and it is the indication of failure. This happened for all the materials investigated.

Journal of Materials in Civil Engineering. Submitted November 20, 2012; accepted March 25, 2013;
posted ahead of print April 1, 2013. doi:10.1061/(ASCE)MT.1943-5533.0000824

Conclusions

The resilient moduli and permanent deformation characteristics of geogrid-reinforced C&D materials were determined to assess the viability of using geogrid reinforced C&D materials as alternative construction materials in pavement applications. RLT tests were undertaken on unreinforced C&D and geogrid-reinforced C&D materials with Biaxial and Triaxial geogrids. The results of the RLT tests were compared between the unreinforced and geogrid-reinforced C&D materials. The RCA and CB materials were tested in the laboratory.

The incorporation of geogrids was found to have significant effects on the resilient modulus and permanent deformation characteristics of C&D materials. The M_R properties of the geogrid-reinforced RCA and CB were found to be higher than that of the respective unreinforced material. The permanent deformation characteristics of geogrid-reinforced RCA and CB were smaller than that of the respective unreinforced material. The M_R value was consistently higher for unreinforced and geogrid-reinforced RCA as compared to the corresponding CB materials for the various confining stresses, indicating RCA to be a higher quality material than CB. Reinforcement of RCA and CB with geogrids was found to result in improved stiffness properties. The M_R value of RCA+Biaxial increased by 24% and of RCA+Triaxial increased by 34% when compared with unreinforced RCA. The permanent deformation value obtained from RCA+Biaxial decreased by 29% and of RCA+Triaxial decreased by 36% when compared with unreinforced RCA. The M_R value of CB+Biaxial increased by 16% and of CB+Triaxial increased by 55% when compared with unreinforced CB. The permanent deformation value decreased by 29% and 37% for CB+Biaxial and CB+Triaxial respectively when compared with unreinforced CB material.

Journal of Materials in Civil Engineering. Submitted November 20, 2012; accepted March 25, 2013; posted ahead of print April 1, 2013. doi:10.1061/(ASCE)MT.1943-5533.0000824

The effects of different deviatoric stress on the resilient modulus test for unreinforced and geogrid-reinforced RCA were investigated by undertaking regression analyses of RLT results using the two and three-parameter models. The regression analysis indicated that the three-parameter resilient modulus model provides an excellent fit for confining and deviatoric stress effect.

The two-parameters ($logk_1$ and k_2) obtained from statistical analysis obtained a very good fit for the unreinforced and geogrid-reinforced RCA and CB. The $logk_1$ parameter was found to vary from 0.26-0.38 and the k_2 parameter values are almost the same which is close to 1 for RCA aggregate. Furthermore, $logk_1$ parameter varies from 0.10 to 0.28 and the k_2 parameter values vary from 0.84 to 0.89 for CB aggregate. The three-parameter model was observed to similarly provide an excellent fit. The structural layer coefficients values for base and subbase layers were calculated from resilient modulus results and found to be higher with geogrid reinforcement. The results also show that the resilient modulus increased with an increase of deviator stress.

Permanent deformation characteristics of geogrid-reinforced RCA and CB were assessed using RLT tests. The results indicate that the permanent strain increased with the increases of each deviator stresses at a constant confining stress. The specimens failed after a certain number of load cycles at 350 kPa deviator stress. The RCA+Triaxial and CB+Triaxial specimens exhibited lower permanent strain as compared to the corresponding Biaxial and unreinforced materials. The lowest permanent strain was obtained for RCA+Triaxial. The deformation characteristics of the unreinforced and reinforced specimens showed that the responses were observed plastic for a finite number of load cycles and after post compaction not much permanent strain was observed in the first two stages.

Journal of Materials in Civil Engineering. Submitted November 20, 2012; accepted March 25, 2013; posted ahead of print April 1, 2013. doi:10.1061/(ASCE)MT.1943-5533.0000824

References

AASHTO. (1993). "Guide for the Design of Pavement Structures". *American Society of State and Highway Transportation Officials, Washington, D.C.*

AASHTO. (2003). "Determining the resilient modulus of soils and aggregate materials". *American society of state and Highway Transportation Officials, Washington, D.C.* T-307-99.

Aatheesan, T., Arulrajah, A., Bo, M.W., Vuong, B. and Wilson, J. (2010). "Crushed brick blends with crushed rock for pavement systems". *Proceedings of the Institution of Civil Engineers, Waste and Resource Management*, 163 (1), 29–35.

Abu-Farsakh, M., Nazzal, M., and Mohammad, L. (2007) "Effect of reinforcement on resilient and permanent deformations of base course material". *Journal of the Transportation Research Board*, No. 2004, Soil Mechanics, 120 - 131.

Alfaro, M.C., Miura, N. and Bergado, D.T. (1995). "Soil geogrid reinforcement interaction by pullout and direct shear tests". *ASTM Geotechnical Testing Journal*, 18 (2), 157–167.

Ali, M.M.Y., Arulrajah, A., Disfani, M.M. and Piratheepan, J. (2011). "Suitability of Using Recycled Glass–Crushed Rock Blends for Pavement Subbase Applications". *Geo-frontiers 2011, Conference on Geotechnical and Foundation Design, American Society of Civil Engineers*, Dallas, TX, 1325–1334.

Apotheker, S. (1990). "Construction and demolition debris – the invisible waste stream". *Resources, Conservation and Recycling*, 9, 66–74.

Arulrajah, A., Piratheepan, J., Aatheesan, T. and Bo, M.W. (2011a). "Geotechnical Properties of Recycled Crushed Brick in Pavement Applications". *Journal of Materials in Civil Engineering, ASCE*, 23 (10), 1444–1542.

Arulrajah, A., Disfani, M.M., Suthagaran, V. and Imteaz, M. (2011b). "Select chemical and engineering properties of wastewater biosolids". *Waste Management,* 31, 2522–2526.

Arulrajah, A., Piratheepan, J., Bo, M.W. and Sivakugan, N. (2012a). "Geotechnical characteristics of recycled crushed brick blends for pavement sub-base applications". *Canadian Geotechnical Journal*, 49 (7), 796-811.

Arulrajah, A., Piratheepan J., Disfani, M.M. and Bo, M.W. (2012b). "Geotechnical and geoenvironmental properties of recycled construction and demolition materials in pavement subbase applications". *Journal of Materials in Civil Engineering, ASCE*, (Article in press).

Arulrajah, A., Piratheepan, J., Ali, M.M.Y. and Bo, M.W. (2012c). "Geotechnical properties of recycled concrete aggregate in pavement sub-base applications", *ASTM Geotechnical Testing Journal*, 35 (5), 1-9.

Arulrajah, A., Ali, M.M.Y., Disfani, M.M., Piratheepan J. and Bo, M.W. (2012d). "Geotechnical performance of recycled glass-waste rock blends in footpath bases". *Journal of Materials in Civil Engineering, ASCE*, (Article in press).

Arulrajah, A., Ali, M.M.Y, Piratheepan, J. and Bo, M.W. (2012e). "Geotechnical properties of waste excavation rock in pavement subbase applications". *Journal of Materials in Civil Engineering, ASCE*, 24 (7), 924–932.

Arulrajah, A., Disfani, M.M., Suthagaran, V. and Bo, M.W. (2013a). "Laboratory evaluation of the geotechnical characteristics of wastewater biosolids in road embankments". *Journal of Materials in Civil Engineering. (Article in press).*

Arulrajah, A., Piratheepan, J., Disfani, M.M. and Bo, M.W. (2013b). "Resilient moduli response of recycled Construction and demolition materials in Pavement subbase applications". *Journal of Materials in Civil Engineering. (Article in press).*

Journal of Materials in Civil Engineering. Submitted November 20, 2012; accepted March 25, 2013; posted ahead of print April 1, 2013. doi:10.1061/(ASCE)MT.1943-5533.0000824

ASTM. (2006). "Standard test method for resistance to degradation of small-size coarse aggregate by abrasion and impact in the Los Angeles machine". *ASTM-C131, West Conshohocken, PA.*

ASTM. (2007). "Standard Test Method for CBR (California Bearing Ratio) of Laboratory-Compacted Soils". ASTM-*D1883-07. West Conshohocken, PA.*

ASTM. (2007). "Standard Test Method for Particle-Size Analysis of Soils". *ASTM-D422-63. West Conshohocken, PA.*

ASTM. (2007). "Standard test methods for moisture, ash, and organic matter of peat and other organic soils". *ASTM-D2974, West Conshohocken, PA.*

ASTM. (2009). "Standard test methods for laboratory compaction characteristics of soil using modified effort". *ASTM-D1557, West Conshohocken, PA.*

Austroads (2004). "Pavement design – A guide to the structural design of road pavements", Austroads Inc..

Azam, A.M. and Cameron, D.A. (2012). "Geotechnical properties of blends of recycled clay masonry and recycled concrete aggregates in unbound pavement construction". *Journal of Materials in Civil Engineering, ASCE* (Article in press).

Bianchini, G., Marrocchino, E., Tassinari, R. and Vaccaro, C. (2005). "Recycling of Construction and Demolition Waste Materials: A Chemical-Mineralogical Appraisal". *Waste Management*, 25, 149–159.

British Standard Institution (BSI). (2000). "Method for determination of particle shape; Flakiness index". *BS812-105.1, London.*

Chen, Q., Abu-Farsakh, M., Voyiadjis, G.Z. and Souci, G. (2012). "Shakedown Analysis of Geogrid-Reinforced Granular Base Material." *Journal of Materials in Civil Engineering. (Article in press)*

Journal of Materials in Civil Engineering. Submitted November 20, 2012; accepted March 25, 2013; posted ahead of print April 1, 2013. doi:10.1061/(ASCE)MT.1943-5533.0000824

Chung, S.S. and Lo, C.W.H. (2003). "Evaluating Sustainability in Waste Management: The Case of Construction and Demolition, Chemical and Clinical Wastes in Hong Kong". *Resources, Conservation and Recycling*, 37, 119–145.

Dawson, A. R. and Wellner, F. (1999). "Plastic Behavior of Granular Materials." *Report ARC Project 933 Reference PRG99014. University of Nottingham, United Kingdom.*

Debieb, F. and Kenai, S. (2008). "The Use of Coarse and Fine Crushed Bricks as Aggregate in Concrete." *Construction and Building Mater*ials, 22, 886–893.

Disfani, M.M., Arulrajah, A., Bo, M.W. and Hankour, R. (2011). "Recycled Crushed Glass in Road Work Applications". *Waste Management,* 31 (11), 2341–2351.

Disfani, M.M., Arulrajah, A., Bo, M.W. and Sivakugan, N. (2012). "Environmental Risks of Using Recycled Crushed Glass in Road Applications". *Journal of Cleaner Production,* 20 (1), 170–179.

Fang-Le, P. and Jian-Zhong, L. (2004). "Modeling of state parameter and hardening function for granular materials." *Journal of Central South University and Technology*, 11 (2), 176–179.

Gabr, A. and Cameron, D. (2012). "Properties of Recycled Concrete Aggregate for Unbound Pavement Construction." *Journal of Materials in Civil Engineering*, ASCE, 24 (6), 754–764.

Gavilan, R.M. and Bernold, L.E. (1994). "Source evaluation of solid waste in building construction". *Journal of Construction Engineering and Management*, 120 (5), 36–52.

Gnanendran, C.T. and Woodburn, L.J. (2003). "Recycled aggregate for pavement construction and the influence of stabilization". *Proc., Conf. of the Australian Road Research Board*, 21, 1755–1768.

Journal of Materials in Civil Engineering. Submitted November 20, 2012; accepted March 25, 2013; posted ahead of print April 1, 2013. doi:10.1061/(ASCE)MT.1943-5533.0000824

Goodhue, M.J., Edil, T.B. and Benson, C.H. (2000). "Interaction of foundry sands with geosynthetics". *Journal of Geotechnical and Geoenvironmental Eng*ineering, ASCE, 127 (4), 353–62.

Han, J., Pokharel, S.K., Yang, X., Manandhar, C., Leshchinsky, D., Halahmi, I., and Parsons, R.L. (2011). "Performance of geocell-reinforced RAP bases over weak subgrade under full-scale moving wheel loads". *Journal of Materials in Civil Engineering*, ASCE, 23 (11), 1525-1534.

Hoyos, L.R., Puppala, A.J. and Ordonez, C.A. (2011). "Characterization of cement fiber-treated reclaimed asphalt pavement aggregates: preliminary investigation". *Journal of Materials in Civil Engineering, ASCE,* 23 (7), 977–989.

Huang, W.L., Lin, D.H., Chang, N.B. and Lin, K.S. (2002). "Recycling of Construction and Demolition Waste via a Mechanical Sorting Process". *Resources, Conservation and Recycling*, 37, 23–37.

Imteaz, M.A., Ali, M.M.Y. and Arulrajah, A. (2012). "Possible environmental impacts of recycled glass used as a pavement base material". *Waste Management & Research*, 30 (9), 917–921.

Indraratna, B., Salim, W. and Christie, D.H. (2002). "Improvement of recycled ballast using geosynthetics". *Rail International*, 33 (4), 20-29.

Indraratna. B. and Salim, W. (2003). "Deformation and degradation mechanism of recycled ballast stabilized with geosynthetics". *Soils and Foundations*, 43 (4), 35-46.

Indraratna, B., Shahin, M.A. and Salim, W. (2005). "Use of geosynthetics for stabilizing recycled ballast in railway track substructures". *Proceedings of NAGS2005/ GRI 19 Cooperative Conference*, 1-15.

Journal of Materials in Civil Engineering. Submitted November 20, 2012; accepted March 25, 2013; posted ahead of print April 1, 2013. doi:10.1061/(ASCE)MT.1943-5533.0000824

Korkiala, T.L. and Dawson, A. (2007). "Relating full-scale pavement rutting to laboratory permanent deformation testing". *International Journal of Pavement Engineering*, 8 (1), 19–28.

Liu, C.N., Zornberg, J.G., Chen, T.C., Ho, Y.H. and Lin, B.H. (2009a). "Behavior of geogrid-sand interface in direct shear mode". *Journal of Geotechnical and Geoenvironmental Engineering*, ASCE, 135 (12), 1863-1871.

Liu, C.N., Ho, Y.H. and Huang, J.W. (2009b). "Large scale direct shear tests of soil/pet-yarn geogrid interfaces". *Geotextiles and Geomembranes*, 27 (1), 19-30.

Liu, X., Scarpas, A., Blaauwendraad, J. and Genske, D.D. (1998). "Geogrid reinforcing of recycled aggregate materials for road construction: Finite Element Investigation". *Transportation Research Record*, 1611, 78-85.

MacGregor, J.A.C., Highter, W.H. and DeGroot, D.J. (1999). "Structural numbers for reclaimed asphalt pavement base and subbase course mixes". *Transportation Research Record*, 1687, 22–28.

Maher, M.H., Gucunski, N. and Papp, W.J. (1997). "Recycled asphalt pavement as a base and sub-base material". *ASTM Special Technical Publication*, 1275, 42-53.

McKelvey, D., Sivakumar, V., Bell, A. and McLaverty, G. (2002). "Shear strength of recycled construction materials intended for use in vibro ground improvement". *Ground Improvement*, 6 (2), 59-68.

Mengelt, M.J., Edil, T.B. and Benson, C.H. (2000). "Reinforcement of Flexible Pavements Using Geocells". *Geo Engineering Report No. 00-04, University of Wisconsin-Madison, Madison, WN.*

Moghaddas-Nejad, F. and Small, J.C. (2003). "Resilient and permanent characteristics of reinforced granular materials by repeated load triaxial tests". *Geotechnical Testing Journal*, 26 (2), 152-166.

Journal of Materials in Civil Engineering. Submitted November 20, 2012; accepted March 25, 2013; posted ahead of print April 1, 2013. doi:10.1061/(ASCE)MT.1943-5533.0000824

Nazzal, M. (2007). "Laboratory Characterization and Numerical Modeling of Geogrid Reinforced Bases in Flexible Pavements". *Ph.D. Dissertation, Louisiana State University*, Baton Rouge, LA.

Perkins, S.W. (2004). "Development of Design Methods for Geosynthetic Reinforced Flexible Pavements". *DTFH61-01-X-00068, U.S. Department of Transportation*, FHWA, Washington, D.C.

Piratheepan, J., Arulrajah, A. and Disfani, M.M. (2013). "Large-scale direct shear testing of recycled construction and demolition materials", Advances in Civil Engineering Materials, ASTM, Vol. 2, No. 1.

Poon, C.S. and Chan, D. (2006a). "Paving Blocks Made with Recycled Concrete Aggregate and Crushed Clay Brick". *Construction and Building Materials,* 20, 569–577.

Poon, C.S. and Chan, D. (2006b). "Feasible Use of Recycled Concrete Aggregates and Crushed Clay Brick as Unbound Road Sub-Base". *Construction and Building Materials,* 20, 578–585.

Puppala, A.J., Hoyos, L.R. and Potturi, A.K. (2011). "Resilient Moduli Response of Moderately Cement-Treated Reclaimed Asphalt Pavement Aggregates". *Journal of Materials in Civil Engineering, ASCE,* 23 (7), 990-998.

Puppala, A.J., Mohammad, L.N. and Allen, A. (1997). "Engineering behavior of lime treated Louisiana subgrade soil". Transportation Research Record 1546, Transportation Research Board, National Academy of Science, Washington, DC, 24–31.

Rao, A., Jha, K.N. and Misra, S. (2007). "Use of Aggregates from Recycled Construction and Demolition Waste in Concrete". *Resources, Conservation and Recycling,* 50, 70–81.

Standards Association of Australia (SAA). (1996). "Method for sampling and testing aggregates - Particle size distribution by sieving". *AS1141.11.*

Journal of Materials in Civil Engineering. Submitted November 20, 2012; accepted March 25, 2013; posted ahead of print April 1, 2013. doi:10.1061/(ASCE)MT.1943-5533.0000824

Standards Association of Australia (SAA). (2000a). "Particle density and water absorption of fine aggregate". *AS1141.5.*

Standards Association of Australia (SAA). (2000b). "Particle density and water absorption of coarse aggregate Weighing-in-water method". *AS1141.6.1.*

Taha, R., Al-Harthy, A., Al-Shamsi, K. and Al-Zubeidi, M. (2002). "Cement stabilization of reclaimed asphalt pavement aggregate for road bases and subbases". *Journal of Materials in Civil Engineering, ASCE,* 14 (3), 239-245.

Tam, V.W.Y. and Tam, C.M. (2007). "Crushed Aggregates Production from Centralized Combined and Individual Waste Sources in Hong Kong". *Construction and Building Materials,* 21, 879–886.

Thakur, J.K., Han, J., Pokharel, S.K. and Parsons, R.L. (2012). "Performance of geocell-reinforced recycled asphalt pavement (RAP) bases over weak subgrade under cyclic plate loading". *Geotextiles and Geomembranes*, 35, 14-24.

Tatlisoz, N., Edil, T.B. and Benson, C.H. (1998). "Interaction between reinforcing geosynthetics and soil-tire chip mixtures". *Journal of Geotechnical and Geoenvironmental Engineering*, *ASCE,* 124 (11), 1109-1119.

Journal of Materials in Civil Engineering. Submitted November 20, 2012; accepted March 25, 2013;
posted ahead of print April 1, 2013. doi:10.1061/(ASCE)MT.1943-5533.0000824

List of Tables

Journal of Materials in Civil Engineering. Submitted November 20, 2012; accepted March 25, 2013;
posted ahead of print April 1, 2013. doi:10.1061/(ASCE)MT.1943-5533.0000824

Table 1: Geotechnical properties of C&D materials

Geotechnical Properties	**Testing Standard**	**RCA**	**CB**
Specific gravity -coarse	AS 1141.5 (2000a)	2.70	2.41
Specific gravity -fine	AS 1141.5 (2000a)	2.60	2.48
Water absorption-coarse (%)	AS 1141.6.1 (2000b)	6.70	13.76
Water absorption-fine (%)	AS 1141.6.1 (2000b)	7.05	10.28
Organic content (%)	ASTM D2974 (2007)	1.80	2.02
Fine content (%)	ASTM D422-63 (2007)	9.90	9.00
Sand content (%)	ASTM D422-63 (2007)	42.2	38.4
Gravel content (%)	ASTM D422-63 (2007)	47.9	52.6
Coefficient curvature (c_c)	ASTM D422-63 (2007)	2.97	2.84
Coefficient uniformity (c_u)	ASTM D422-63 (2007)	78.83	41.05
Flakiness index	BS 812-105.1 (2000)	12.83	13.75
Los Angeles abrasion loss	ASTM C131 (2006)	30.50	34.50
Max dry density (Mg/m^3)	ASTM D1557 (2009)	2.08	2.04
Optimum moisture content (%)	ASTM D1557 (2009)	12.5	12.75
California Bearing Ratio (%)	ASTM D1883 (2007)	172	135

Journal of Materials in Civil Engineering. Submitted November 20, 2012; accepted March 25, 2013;
posted ahead of print April 1, 2013. doi:10.1061/(ASCE)MT.1943-5533.0000824

Table 2: Two-parameter bulk stress coefficients

Specimen type	$Log\ k_1$	k_1	k_2	R^2
RCA	0.26	1.82	0.80	0.98
RCA+Biaxial	0.28	1.91	0.88	0.98
RCA+Triaxial	0.38	2.40	0.95	0.99
CB	0.10	1.26	0.84	0.97
CB+Biaxial	0.14	1.37	0.85	0.98
CB+Triaxial	0.28	1.92	0.89	0.98

Journal of Materials in Civil Engineering. Submitted November 20, 2012; accepted March 25, 2013;
posted ahead of print April 1, 2013. doi:10.1061/(ASCE)MT.1943-5533.0000824

Table 3: Three-parameter resilient modulus coefficients

Specimen type	k_3	k_4	k_5	R^2
RCA	0.81	0.69	0.12	0.98
RCA+Biaxial	0.96	0.73	0.14	0.99
RCA+Triaxial	1.10	0.70	0.15	0.99
CB	0.75	0.35	0.08	0.99
CB+Biaxial	0.88	0.37	0.10	0.98
CB+Triaxial	1.04	0.38	0.10	0.99

Journal of Materials in Civil Engineering. Submitted November 20, 2012; accepted March 25, 2013;
posted ahead of print April 1, 2013. doi:10.1061/(ASCE)MT.1943-5533.0000824

Table 4: Structural coefficient "a_2" for base layer

Confine stress (kPa)	**20.70**	**34.5**	**68.9**	**103.4**	**137.9**
RCA	0.025	0.068	0.124	0.144	0.171
RCA+Biaxial	0.047	0.087	0.149	0.168	0.198
RCA+Triaxial	0.059	0.100	0.159	0.180	0.205
CB	0.028	0.033	0.090	0.106	0.129
CB+Biaxial	0.033	0.050	0.104	0.117	0.147
CB+Triaxial	0.035	0.076	0.135	0.156	0.181

Journal of Materials in Civil Engineering. Submitted November 20, 2012; accepted March 25, 2013;
posted ahead of print April 1, 2013. doi:10.1061/(ASCE)MT.1943-5533.0000824

Table 5: Structural coefficient "a_3" for sub-base layer

Confine stress (kPa)	**20.70**	**34.5**	**68.9**	**103.4**	**137.9**
RCA	0.074	0.114	0.165	0.183	0.208
RCA+Biaxial	0.095	0.131	0.187	0.205	0.232
RCA+Triaxial	0.106	0.143	0.197	0.216	0.239
CB	0.03	0.08	0.13	0.15	0.17
CB+Biaxial	0.04	0.10	0.15	0.16	0.19
CB+Triaxial	0.08	0.12	0.17	0.19	0.22

Journal of Materials in Civil Engineering. Submitted November 20, 2012; accepted March 25, 2013;
posted ahead of print April 1, 2013. doi:10.1061/(ASCE)MT.1943-5533.0000824

Table 6: Permanent strain (microstrain) of geogrid reinforced C&D materials

Deviator stresses	**150kPa**	**250kPa**	**350kPa**
RCA	11742.3	16077.8	Failed
RCA+Biaxial	8293.4	15994.4	Failed
RCA+Triaxial	7478.6	15070.1	Failed
CB	12519.4	19552.1	Failed
CB+Biaxial	8858.41	17025.23	Failed
CB+Triaxial	7849.9	15861.8	Failed

Journal of Materials in Civil Engineering. Submitted November 20, 2012; accepted March 25, 2013;
posted ahead of print April 1, 2013. doi:10.1061/(ASCE)MT.1943-5533.0000824

List of Figures

Figure 1

Journal of Materials in Civil Engineering. Submitted November 20, 2012; accepted March 25, 2013;
posted ahead of print April 1, 2013. doi:10.1061/(ASCE)MT.1943-5533.0000824

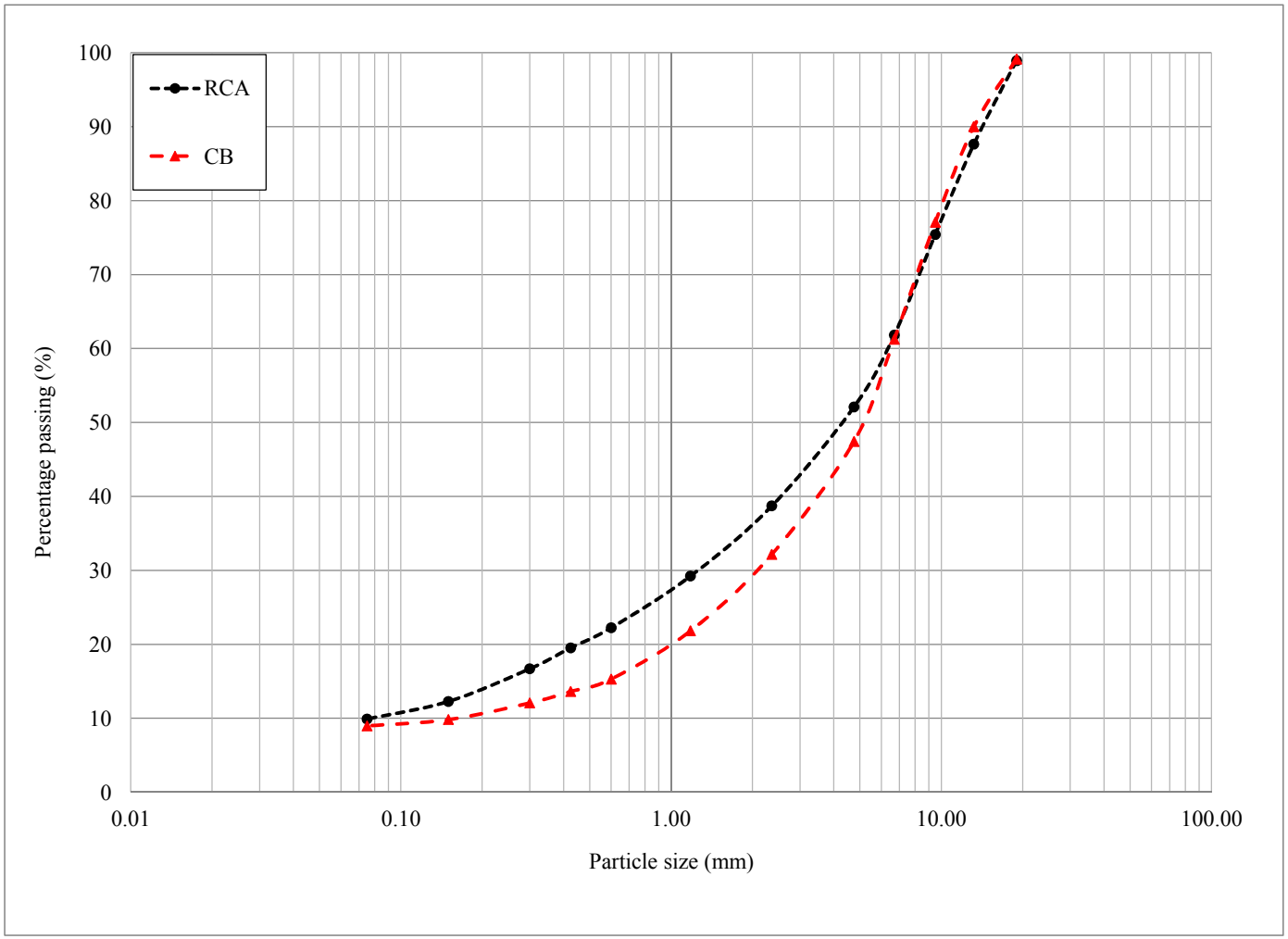

Figure 2

Journal of Materials in Civil Engineering. Submitted November 20, 2012; accepted March 25, 2013;
posted ahead of print April 1, 2013. doi:10.1061/(ASCE)MT.1943-5533.0000824

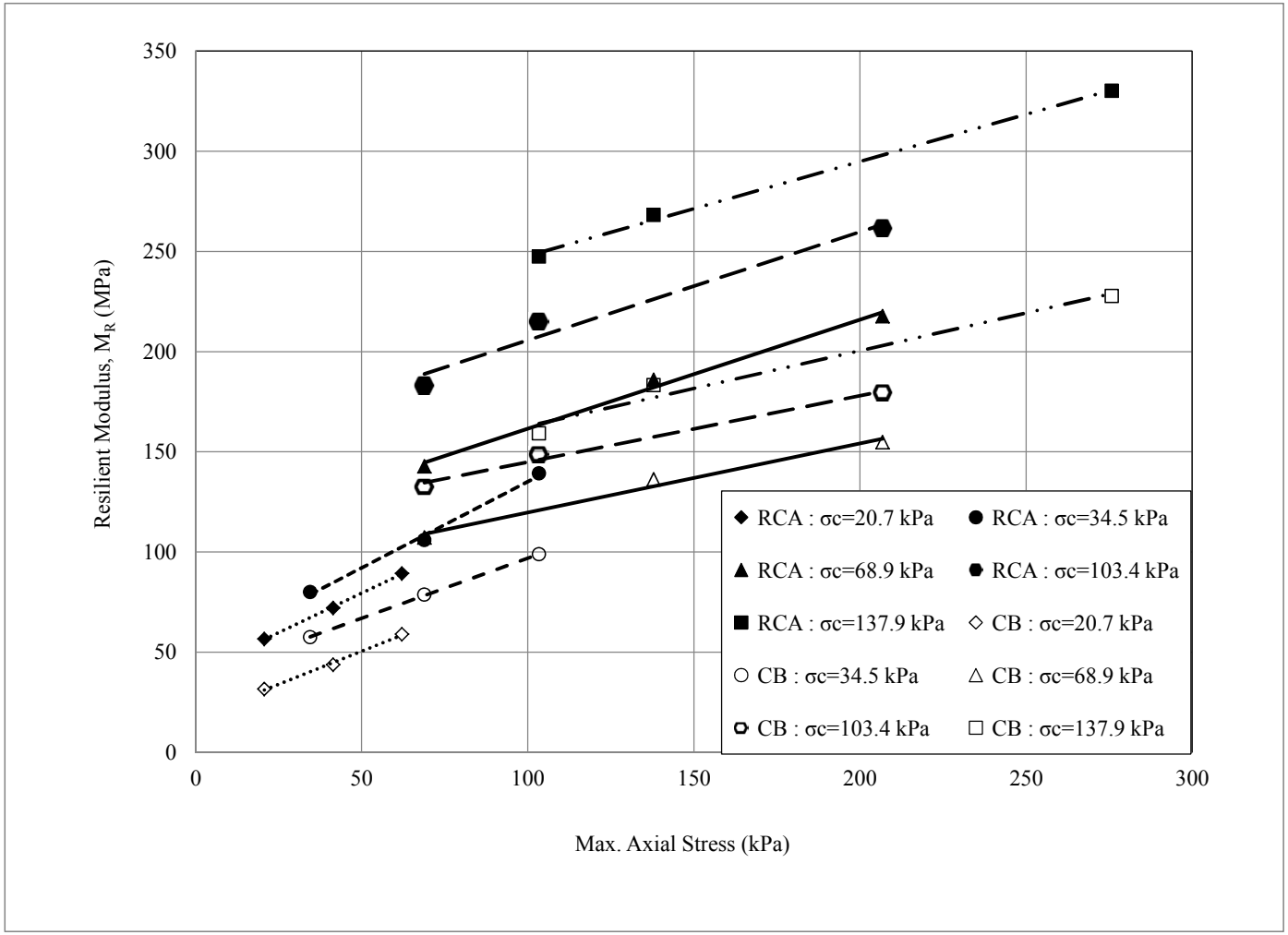

Figure 3

Journal of Materials in Civil Engineering. Submitted November 20, 2012; accepted March 25, 2013;
posted ahead of print April 1, 2013. doi:10.1061/(ASCE)MT.1943-5533.0000824

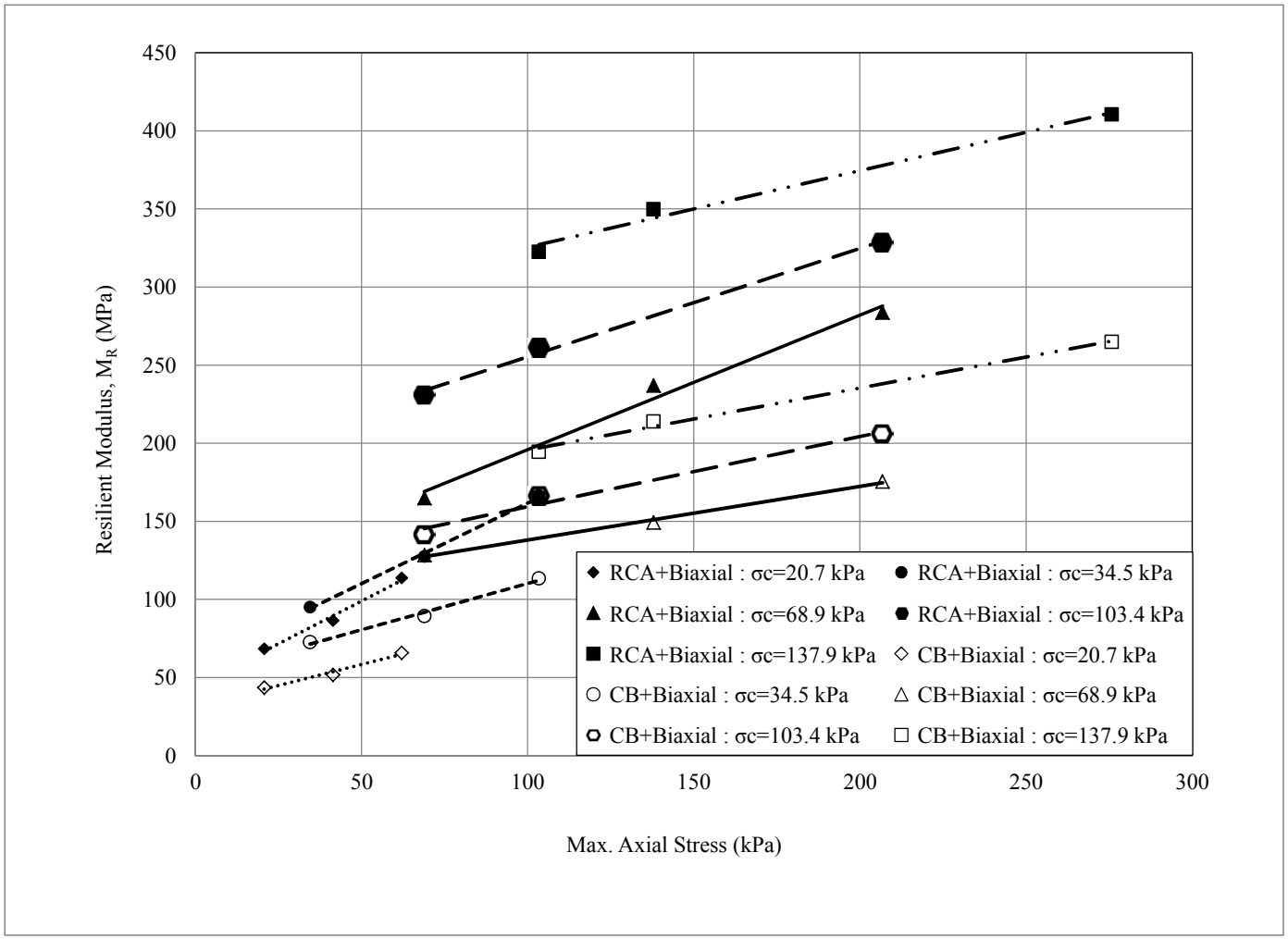

Figure 4

Journal of Materials in Civil Engineering. Submitted November 20, 2012; accepted March 25, 2013;
posted ahead of print April 1, 2013. doi:10.1061/(ASCE)MT.1943-5533.0000824

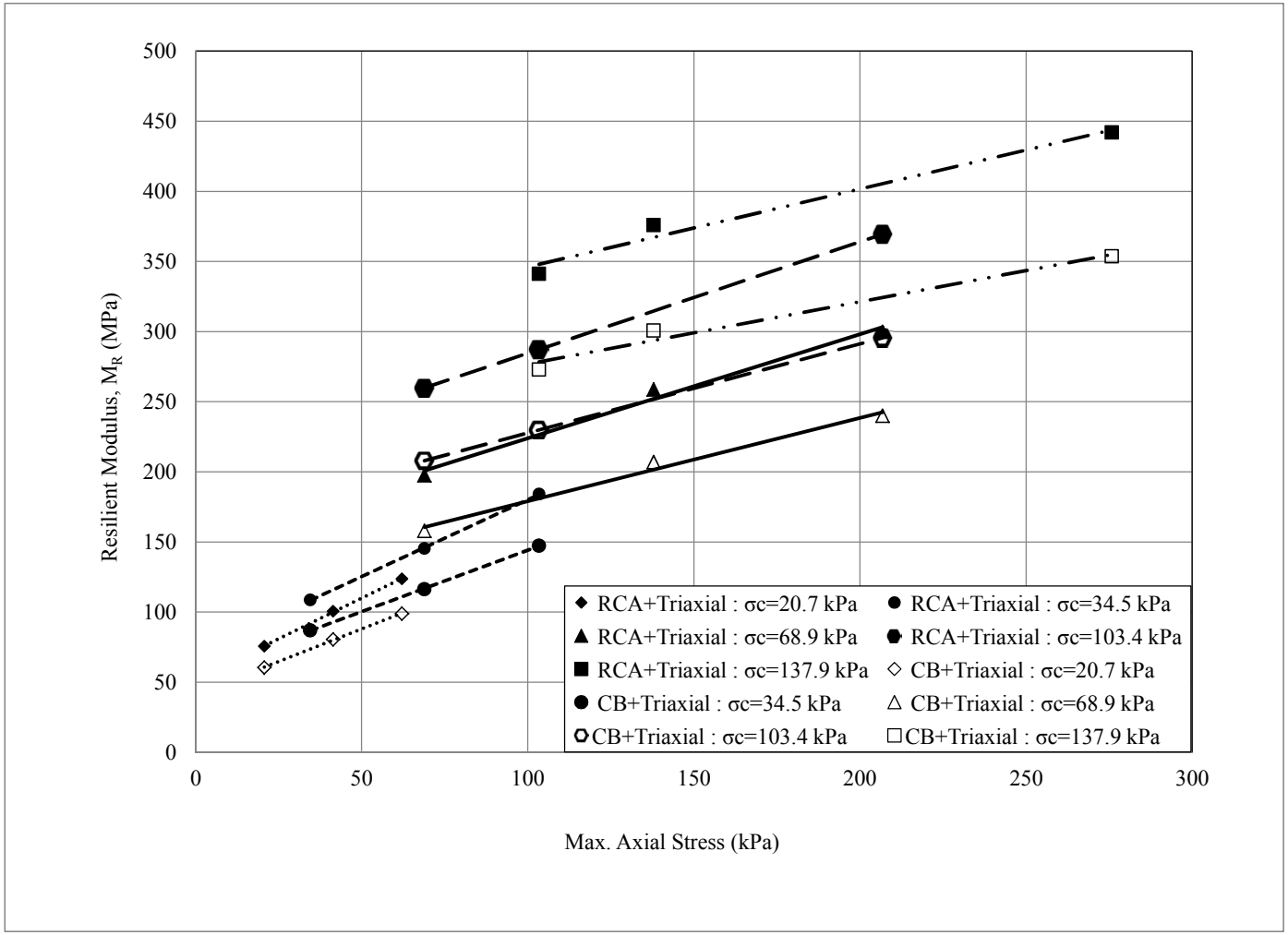

Figure 5

Journal of Materials in Civil Engineering. Submitted November 20, 2012; accepted March 25, 2013;
posted ahead of print April 1, 2013. doi:10.1061/(ASCE)MT.1943-5533.0000824

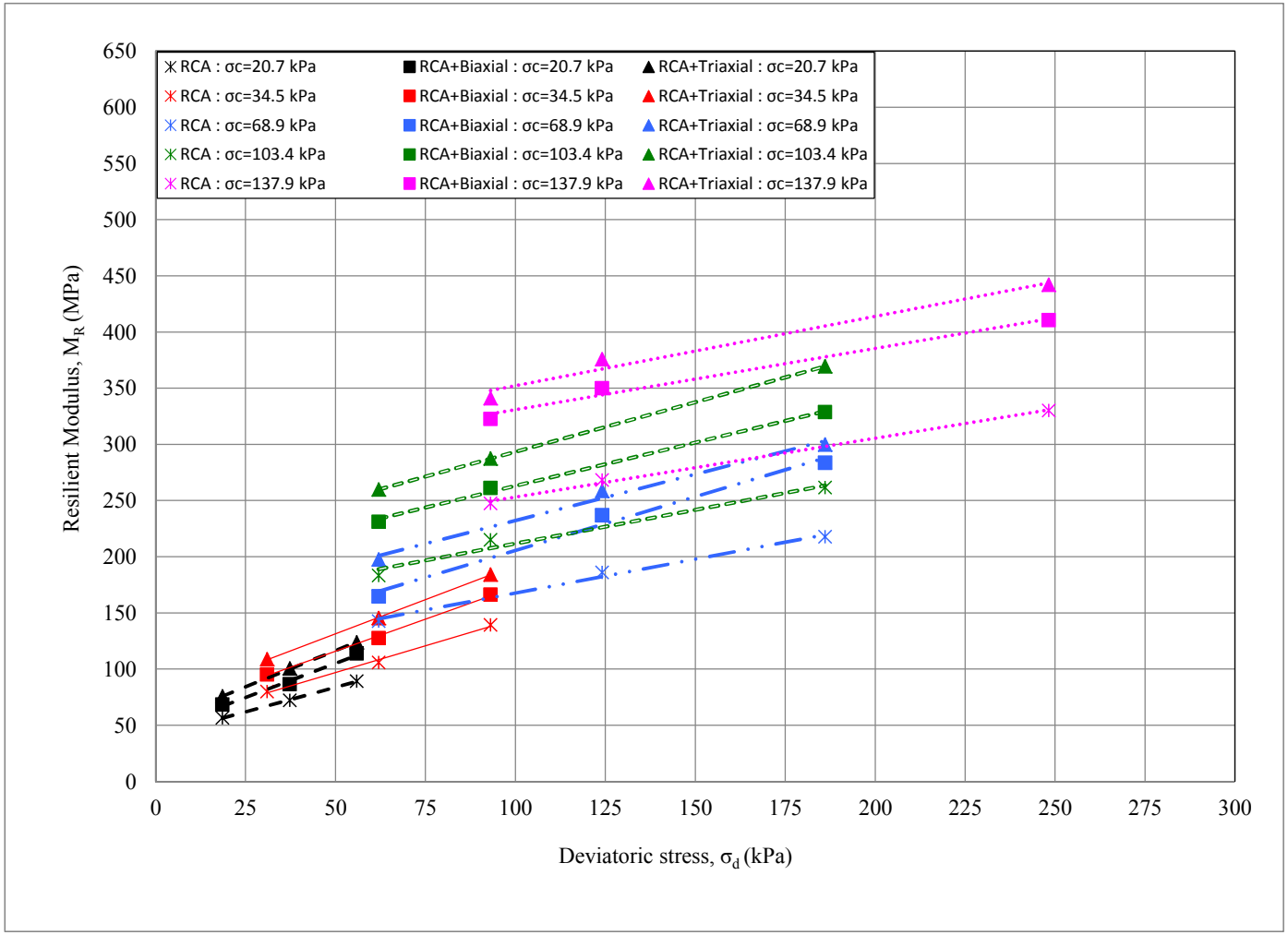

Figure 6

Journal of Materials in Civil Engineering. Submitted November 20, 2012; accepted March 25, 2013;
posted ahead of print April 1, 2013. doi:10.1061/(ASCE)MT.1943-5533.0000824

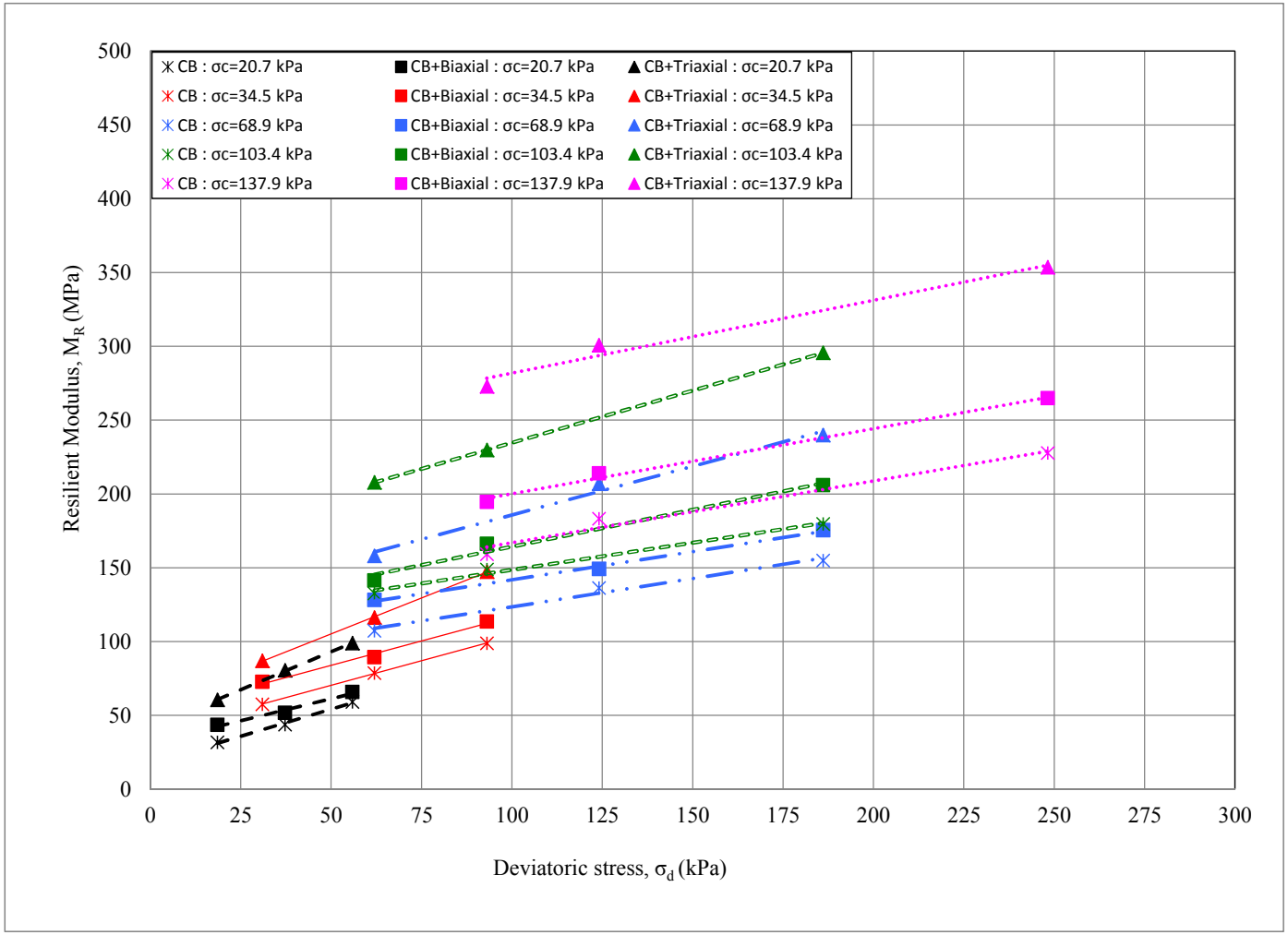

Figure 7

Journal of Materials in Civil Engineering. Submitted November 20, 2012; accepted March 25, 2013;
posted ahead of print April 1, 2013. doi:10.1061/(ASCE)MT.1943-5533.0000824

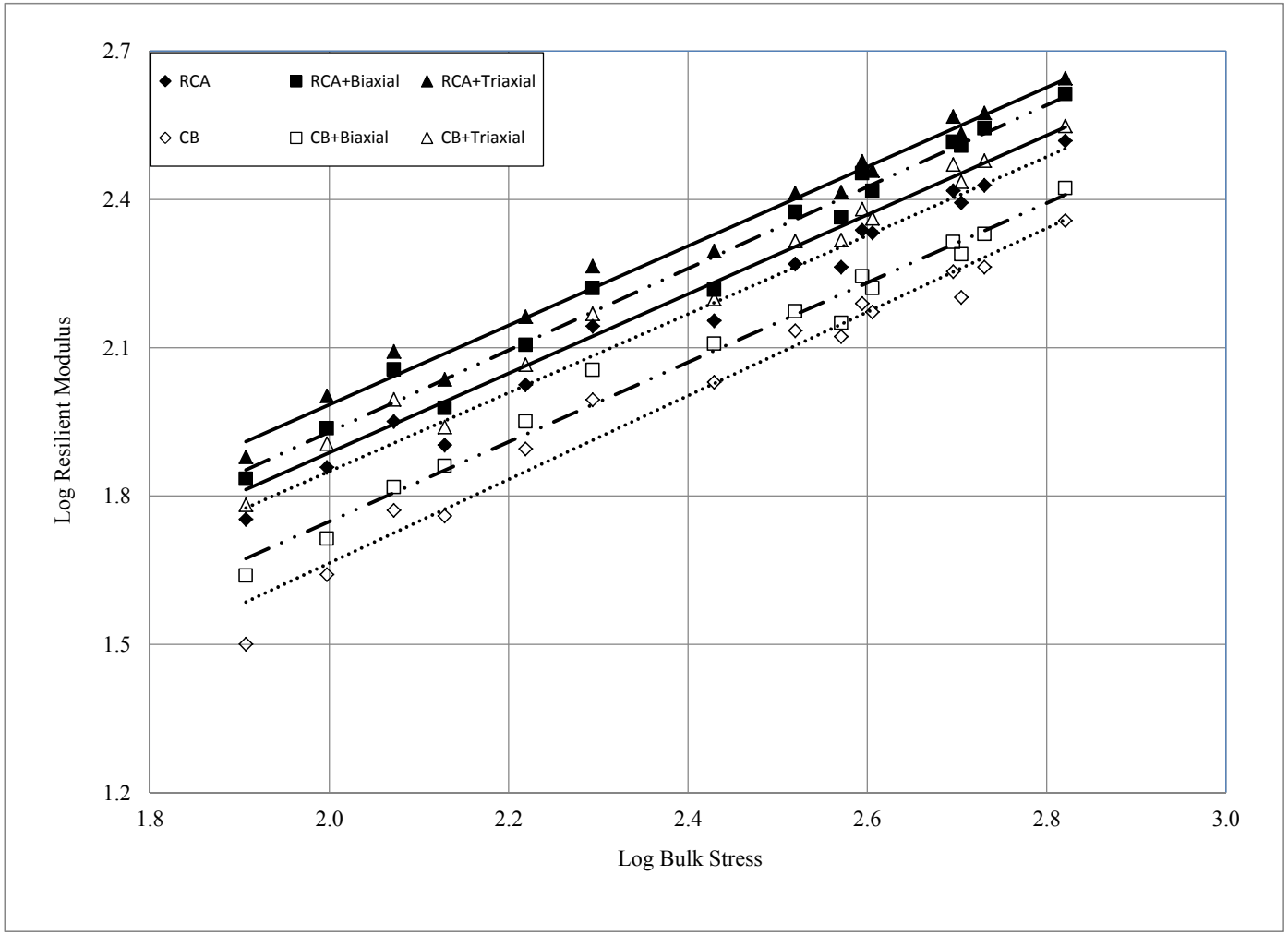

Figure 8

Journal of Materials in Civil Engineering. Submitted November 20, 2012; accepted March 25, 2013;
posted ahead of print April 1, 2013. doi:10.1061/(ASCE)MT.1943-5533.0000824

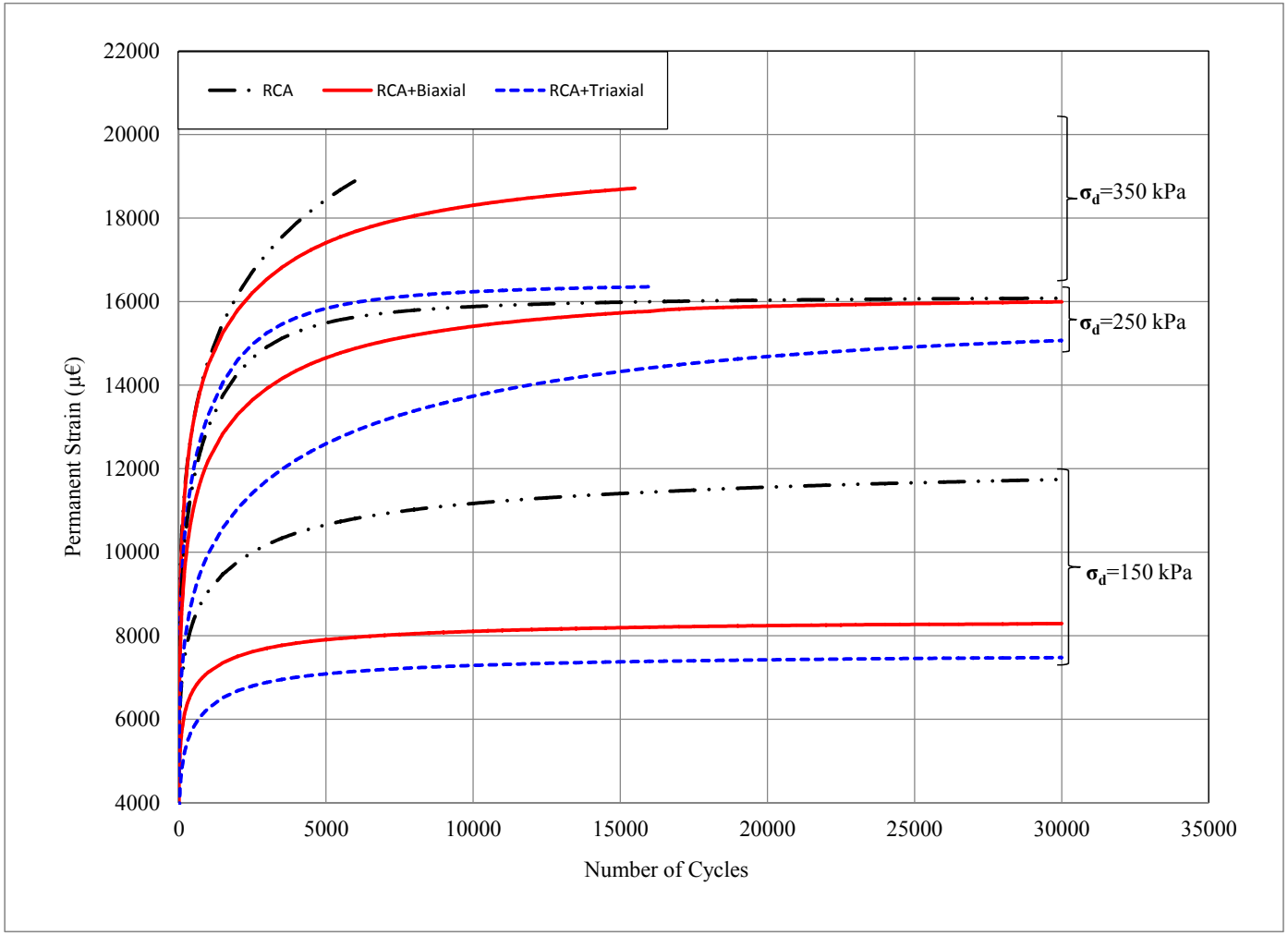

Figure 9

Journal of Materials in Civil Engineering. Submitted November 20, 2012; accepted March 25, 2013;
posted ahead of print April 1, 2013. doi:10.1061/(ASCE)MT.1943-5533.0000824

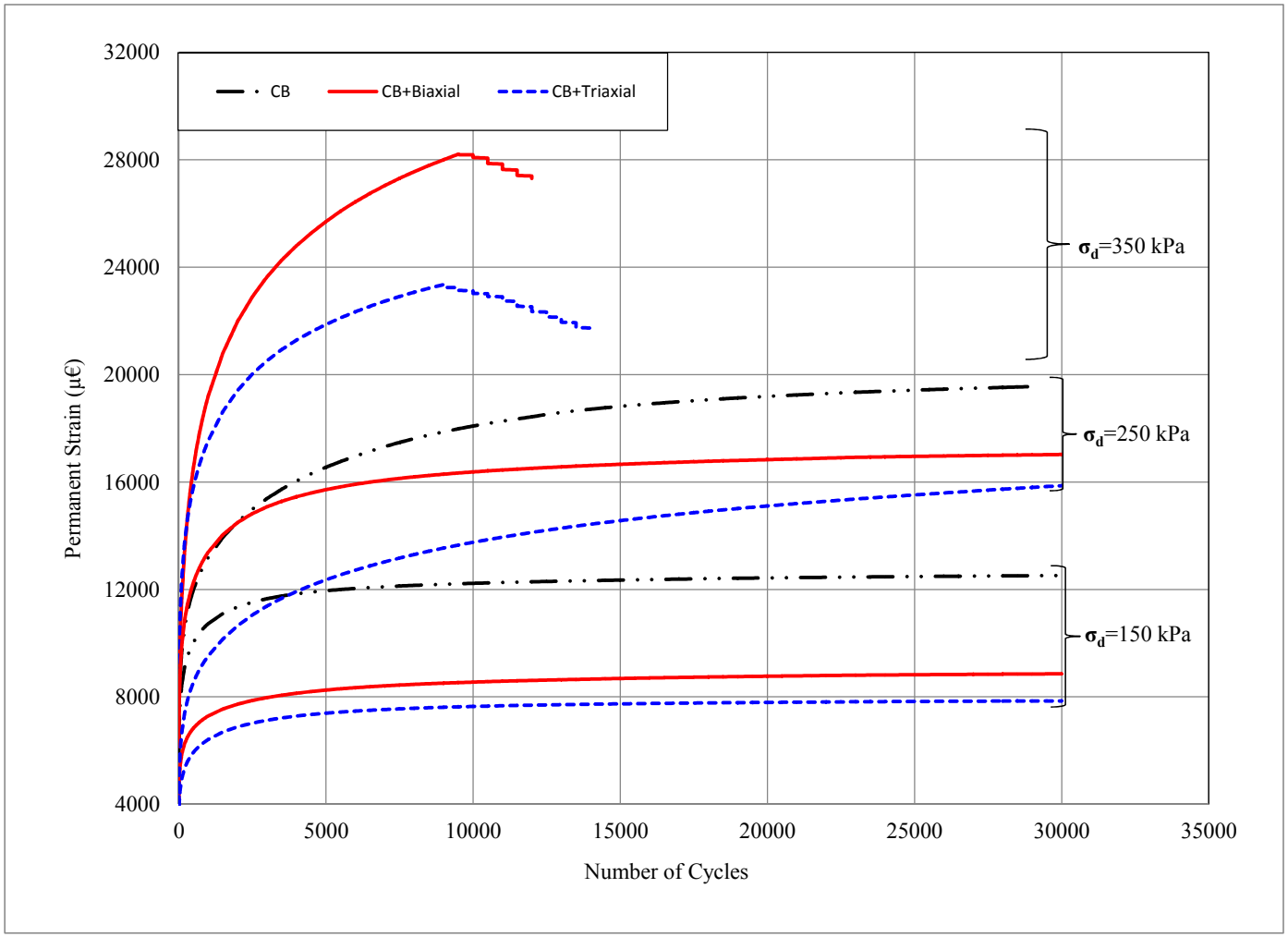

Figure 10

Journal of Materials in Civil Engineering. Submitted November 20, 2012; accepted March 25, 2013;
posted ahead of print April 1, 2013. doi:10.1061/(ASCE)MT.1943-5533.0000824

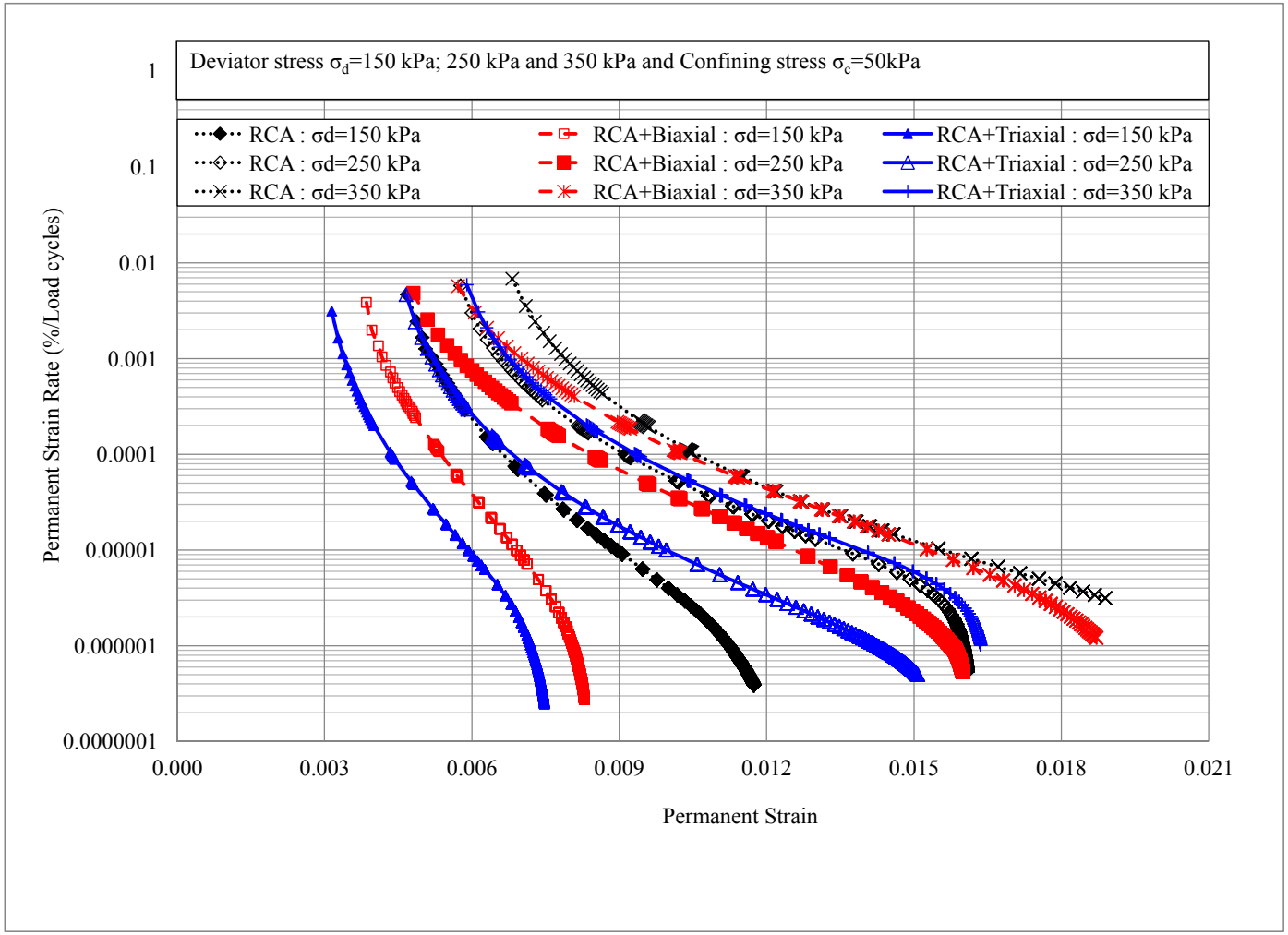

Figure 11

Journal of Materials in Civil Engineering. Submitted November 20, 2012; accepted March 25, 2013;
posted ahead of print April 1, 2013. doi:10.1061/(ASCE)MT.1943-5533.0000824